Kinetic and Thermodynamic Analysis of Induced-Fit Molecular Recognition between Tetraarylporphyrin and Ubiquinone Analogues

Takashi Hayashi,* Tomohito Asai, Frieder M. Borgmeier, Hirohisa Hokazono, and Hisanobu Ogoshi*

Abstract: *meso*-Tetrakis(2-hydroxy-4-nonylphenyl)porphyrin (**1**), which was prepared as a host molecule for ubiquinone analogues, comprises four atropisomers, $\alpha\alpha\alpha\alpha$, $\alpha\alpha\alpha\beta$, $\alpha\alpha\beta\beta$, and $\alpha\beta\alpha\beta$, in a statistical ratio of 1:4:2:1, respectively. The atropisomerization is due to internal rotation about the C(aryl)–C(porphyrin) bonds and is observed even at room temperature. A rate constant for the rotation was determined ($k = 1.73 \times 10^{-5}\ s^{-1}$ in $CHCl_3$ at 25 °C). UV/visible spectrophotometric titration of tetramethoxy-*p*-benzoquinone (**3**) against $\mathbf{1}_{\alpha\alpha\alpha\alpha}$ or $\mathbf{1}_{\alpha\alpha\alpha\beta}$ in $CHCl_3$ at 25 °C showed 1:1 complexation with association constants of $(9.4 \pm 0.1) \times 10^3$ and $(3.5 \pm 0.1) \times 10^2\ M^{-1}$, respectively. Upon addition of **3** to a solution of **1** in $CDCl_3$, the proportion of $\mathbf{1}_{\alpha\alpha\alpha\alpha}$ in the atropisomeric mixture increased and that of the other three isomers decreased over 500 h. At equilibrium the proportion of $\mathbf{1}_{\alpha\alpha\alpha\alpha}$ reached 78% in the presence of **3** (3 equiv); this showed that atropisomerization is induced by complexation with **3**. An atropisomeric shift to $\mathbf{1}_{\alpha\alpha\alpha\alpha}$ was also observed upon addition of 2,3-dimethoxy-*p*-benzoquinone (**4**); however, the proportion of $\mathbf{1}_{\alpha\alpha\alpha\alpha}$ was only 30% at equilibrium, since the difference in binding affinities between $\mathbf{1}_{\alpha\alpha\alpha\alpha}$–**4** and $\mathbf{1}_{\alpha\alpha\alpha\beta}$–**4** complexes is relatively small compared with that between $\mathbf{1}_{\alpha\alpha\alpha\alpha}$–**3** and $\mathbf{1}_{\alpha\alpha\alpha\beta}$–**3** complexes. Nickel and zinc porphyrins, **1**·**Ni** and **1**·**Zn**, also showed induced-fit interaction with **3**. The atropisomeric shift to $\mathbf{1}_{\alpha\alpha\alpha\alpha}$·**Ni** upon addition of **3** was completed within 1 h, whereas guest-induced atropisomerization in **1**·**Zn** was much slower than in free base **1**. The observed changes in the relative amounts of the four atropisomers are identical with the simulated changes calculated from multiple equilibrium systems by use of kinetic and thermodynamic parameters. This system is a suitable model for induced-fit molecular recognition in flexible enzymes.

Keywords: atropisomerism · molecular recognition · porphyrinoids · quinones

Introduction

Over the last two decades a number of chemists have investigated synthetic host–guest systems in order to clarify the behavior of specific protein–ligand binding in biological systems. These model studies have indicated that host molecules with rigid, preorganized structures have good affinity and specificity for guest molecules, owing to the minimal entropy loss of the host molecule upon binding (Scheme 1a).[1] However, structural changes in biological receptors and/or substrates are often required for signal transfer to an active site in proteins, or to initiate catalytic reactions in enzymes. Koshland has suggested that in flexible enzymes the conformational changes induced by substrate binding play an important role in the proper alignment of catalytic active sites with the substrate.[2] This concept was supported by X-ray crystallographic analysis of enzymes, which indicated that internal rotation about a specific bond in the protein molecule took place upon binding between protein and ligand.[3] Thus it is particularly important to evaluate the guest-induced structural changes in flexible biomolecules by use of a variety of artificial receptors (Scheme 1b).[4]

As an example of a new host–guest system capable of induced-fit molecular recognition, we have focused on the atropisomerization of *meso*-tetrakis(2-hydroxy-4-nonylphenyl)porphyrin (**1**) as a host molecule for ubiquinone analogues.[5] In this host, atropisomeric interconversion results from internal rotation about four C(aryl)–C(porphyrin) bonds, even at room temperature.[6, 7] Consequently, four atropisomers, $\mathbf{1}_{\alpha\alpha\alpha\alpha}$, $\mathbf{1}_{\alpha\alpha\alpha\beta}$, $\mathbf{1}_{\alpha\alpha\beta\beta}$, and $\mathbf{1}_{\alpha\beta\alpha\beta}$, are formed in the

[*] Prof. T. Hayashi,[+] Prof. H. Ogoshi[++], T. Asai, F. M. Borgmeier, H. Hokazono
Department of Synthetic Chemistry and Biological Chemistry
Graduate School of Engineering, Kyoto University
Kyoto 606-8501 (Japan)

[+] Current address: Department of Chemistry and Biochemistry
Graduate School of Engineering, Kyushu University
Higashi-ku, Fukuoka 812-8581 (Japan)
Fax: (+81) 92-642-3611
E-mail: thayatcm@mbox.nc.kyushu-u.ac.jp

[++] Current address: Fukui National College of Technology
Sabae 916-8507 (Japan)
E-mail: ogoshi@azalea1.ip.fukui-nct.ac.jp

0947-6539/98/0407-1266 $ 17.50+.50/0

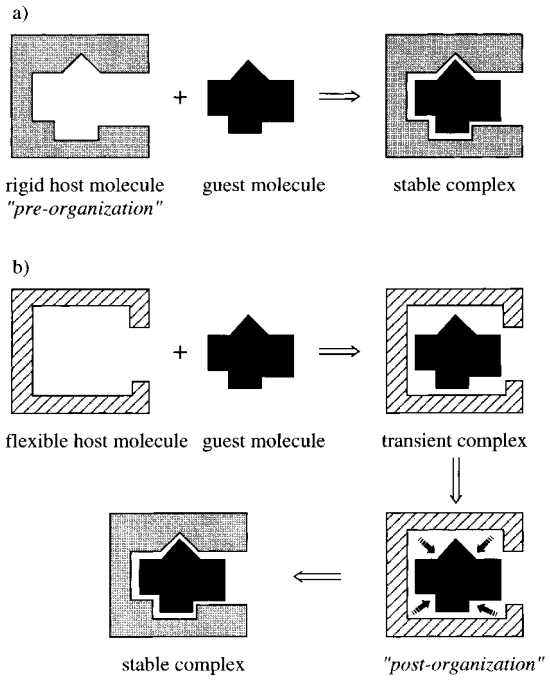

Scheme 1. a) Preorganization and b) postorganization mechanisms in host–guest complexation.

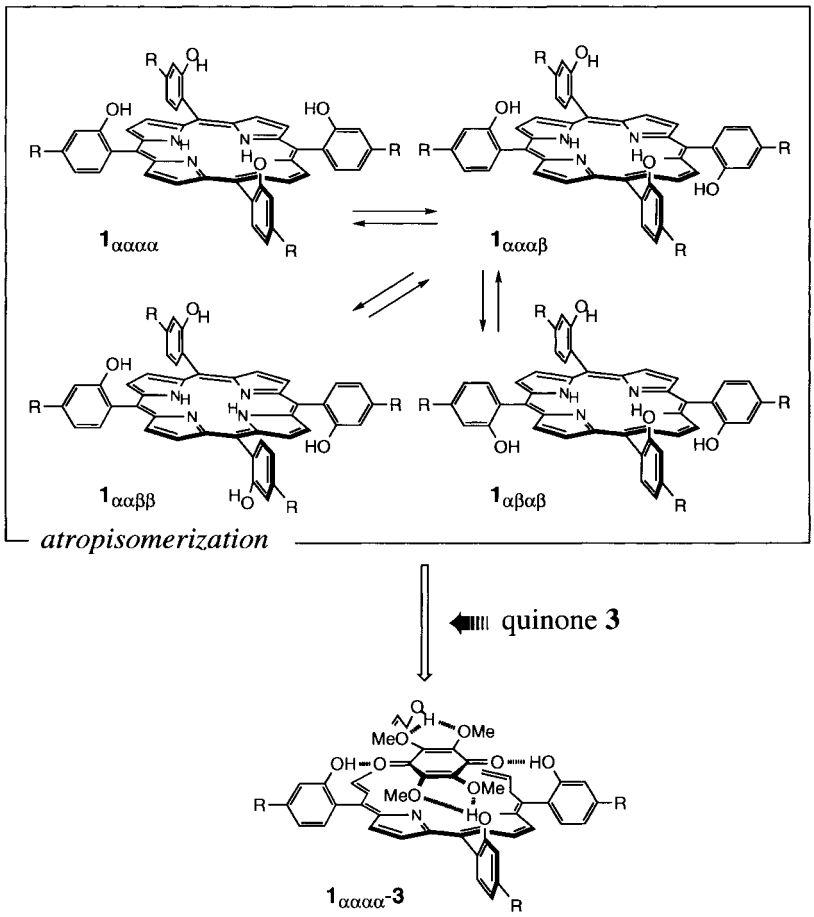

Scheme 2. The atropisomeric interconversion of porphyrin **1** and the mechanism of the shift in equilibrium to $\mathbf{1}_{\alpha\alpha\alpha\alpha}$ upon addition of quinone **3**.

statistical ratio of 1:4:2:1 at equilibrium, where α and β represent the location of the *ortho*-substituent above and below the plane of the porphyrin ring, respectively (Scheme 2).[7] Previously, porphyrin **1** had not been regarded as a suitable host molecule for quinone derivatives, because of its flexible framework. However, we found a dynamic recognition event between **1** and tetramethoxy-*p*-benzoquinone (**3**), in which the equilibrium of the four atropisomers of porphyrin **1** was shifted to the $\mathbf{1}_{\alpha\alpha\alpha\alpha}$ isomer as shown in Scheme 2.[6] In 1980, Elliot and Lindsey separately reported the atropisomerization of *meso*-tetrakis(2-aminophenyl)porphyrin on silica gel. This substrate converted a mixture of atropisomers to the $\alpha\alpha\alpha\alpha$-isomer in 60–70% yield.[8–10] To our knowledge, the present system is the first example of atropisomeric interconversion to the $\alpha\alpha\alpha\alpha$-isomer by induced-fit molecular recognition in homogeneous solution.[6, 11] Here, we wish to report the dynamic process of molecular recognition between **1** or its metal complexes and ubiquinone derivatives. The atropisomerization of host porphyrin induced by the quinone molecule can be completely described with two parameters, a rate constant for internal rotation and an association constant between host and guest. This system is potentially a useful model for investigating quantitatively the rearrangement (*post-organization*) of the host molecule consequent upon host–guest pairing as shown in Scheme 1b.

Abstract in Japanese:

メソテトラキス（2-ヒドロキシ-4-ノニルフェニル）ポルフィリンはポルフィリン環とアリル基間の炭素－炭素結合が室温でも十分に早く回転する結果、4つのアトロプ異性体は平衡状態で1:4:2:1の比で存在している。その中でも特にポルフィリン環に対して水酸基がすべて同一方向に位置するαααα-体、一つの水酸基が反転したααβ-体はそれぞれテトラメトキシ-*p*-ベンゾキノンと9.4 x 10^3 M^{-1}及び3.5 x 10^2 M^{-1} (25 °C, $CHCl_3$) を得た。4つの異性体が平衡状態で存在するクロロホルム溶液にキノンを添加すると、時間とともに異性体比の変化が見られ、約500 時間後にαααα-体が11% から78%に増加し、残りの3つの異性体の濃度が急激に減少していることがNMR 測定から認められた。一方ポルフィリンに対して結合力の弱い2,3-ジメトキシ-*p*-ベンゾキノン を用いた場合、αααα-体比の大きな増加は観測されず、この適合型認識は各々のポルフィリンとキノンとの相互作用における結合定数の差に誘導されることが明らかとなった。さらにポルフィリンのニッケル及び亜鉛錯体を用いて同様の実験を行ったところ、ニッケル錯体の場合αααα-体への極めて早い増加が見られ、亜鉛錯体の場合はαααα-体への異性化は起こるもののその速度はフリーベースよりも極めて遅いことが判明した。これらはテトラアリルポルフィリンの内部回転速度に反映している。この動的認識挙動をそれぞれの結合定数と回転速度定数を用いてシミュレーションした結果、実験値と極めて良い一致が見られ、ポルフィリンのアトロプ異性化を伴う構造変化はキノンの構造に誘起され、最も安定なαααα-体へ平行がずれることが示された。

Results and Discussion

Host molecule: The synthetic route to porphyrin **1** is shown in Scheme 3. To increase the solubility of **1** in organic solvents,

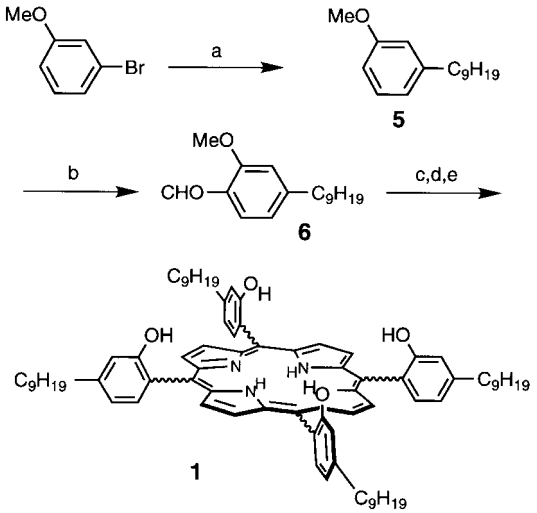

Scheme 3. Synthesis of porphyrin **1** from 3-bromoanisole; reagents and conditions: a) *n*-$C_9H_{19}MgBr$, $NiCl_2$(dppp); b) Cl_2CHOCH_3, $TiCl_4$; c) pyrrole, $BF_3 \cdot OEt_2$; d) 2,3-dichloro-5,6-dicyano-1,4-benzoquinone; e) BBr_3.

four long alkyl chains were substituted at the *para*-position of the aryl groups by a cross-coupling reaction in the presence of [1,3-bis(diphenylphosphino)propane]nickel(II) dichloride as a catalyst.[12] Condensation of pyrrole with 2-methoxy-4-nonylbenzaldehyde, followed by deprotection of the four methyl groups by BBr_3, led to a mixture of the four atropisomers of **1**. Atropisomerization of **1** occurred rapidly through rotation about the C(aryl)–C(porphyrin) bonds and the relative amounts of the four atropisomers, $\mathbf{1}_{\alpha\alpha\alpha\alpha}$ (10.5%), $\mathbf{1}_{\alpha\alpha\alpha\beta}$ (54.0%), $\mathbf{1}_{\alpha\alpha\beta\beta}$ (24.0%), and $\mathbf{1}_{\alpha\beta\alpha\beta}$ (11.5%), were determined by analytical HPLC (Figure 1). Although pure atropisomers

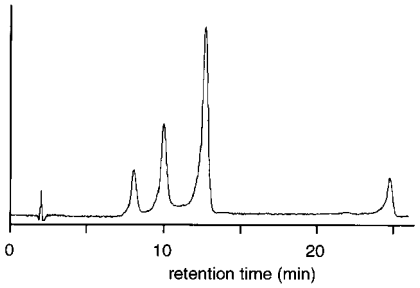

Figure 1. HPLC analysis of a mixture of atropisomers **1** at equilibrium. YMC-packed column AQ-312 (reversed phase); eluent, MeOH/*iso*-PrOH = 65:35–20:80 (1 mL min^{-1}), monitored by UV/vis spectroscopy (420 nm). The relative amounts of the four atropisomers and the respective retention times are as follows: $\mathbf{1}_{\alpha\alpha\alpha\alpha}$, 10.5% (24.8 min); $\mathbf{1}_{\alpha\alpha\alpha\beta}$, 54.0% (12.6 min); $\mathbf{1}_{\alpha\alpha\beta\beta}$, 24.0% (10.0 min); $\mathbf{1}_{\alpha\beta\alpha\beta}$, 11.6% (7.95 min).

could not be isolated at room temperature, the most polar isomer, $\mathbf{1}_{\alpha\alpha\alpha\alpha}$, was isolated by preparative TLC at 4 °C. The rate of isomerization of $\mathbf{1}_{\alpha\alpha\alpha\alpha}$ to the other isomers through rotation of the aryl ring is depicted in Figure 2. The decay of $\mathbf{1}_{\alpha\alpha\alpha\alpha}$ followed first-order kinetics. The rate constant for rotation about one C(aryl)–C(porphyrin) bond was determined from least-squares fitting; $k = (1.73 \pm 0.04) \times 10^{-5}$ s^{-1} in $CHCl_3$ at 25 °C.[13]

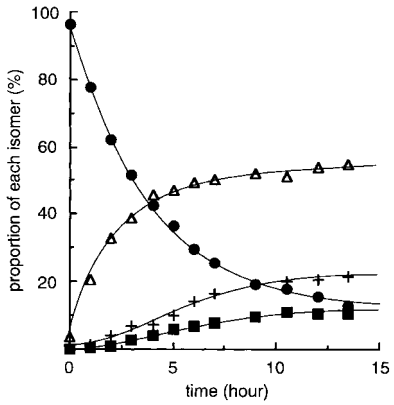

Figure 2. Kinetics of atropisomerization from $\mathbf{1}_{\alpha\alpha\alpha\alpha}$ to the other three isomers in $CHCl_3$ at 25 °C, monitored by HPLC. $\mathbf{1}_{\alpha\alpha\alpha\alpha}$ (●), $\mathbf{1}_{\alpha\alpha\alpha\beta}$ (△), $\mathbf{1}_{\alpha\alpha\beta\beta}$ (+), $\mathbf{1}_{\alpha\beta\alpha\beta}$ (■).

Intermolecular interaction between porphyrin 1 and quinone: Titrimetric measurement by UV/visible absorption spectroscopy demonstrated simple 1:1 complexation between $\mathbf{1}_{\alpha\alpha\alpha\alpha}$ and **3** or $\mathbf{1}_{\alpha\alpha\alpha\beta}$ and **3** with several isosbestic points. The interaction features in the porphyrin–quinone complex were also monitored by ^{1}H NMR spectroscopy. Addition of **3** (4 equiv) to a solution of $\mathbf{1}_{\alpha\alpha\alpha\alpha}$ or $\mathbf{1}_{\alpha\alpha\alpha\beta}$ in $CDCl_3$ resulted in a 1.7–1.9 ppm downfield shift of the signal from the OH protons, owing to hydrogen bonding, whereas the signal from the MeO protons in **3** shifted upfield slightly (ca. −0.16 ppm), owing to the diamagnetic ring current of the aromatic host **1**. These results are consistent with previous data on the binding between *meso*-$\alpha\alpha\alpha\alpha$-tetrakis(2-hydroxy-1-naphthyl)porphyrin (**2**) and **3**.[5] It is clear that hosts $\mathbf{1}_{\alpha\alpha\alpha\alpha}$ and $\mathbf{1}_{\alpha\alpha\alpha\beta}$ form cofacial complexes with **3** through hydrogen bonding.

The association constants and thermodynamic parameters for the porphyrin–quinone complexes are shown in Table 1. The host porphyrins $\mathbf{1}_{\alpha\alpha\alpha\alpha}$ and $\mathbf{1}_{\alpha\alpha\alpha\beta}$ have four and three OH

Table 1. Association constants and thermodynamic parameters for **1**–**3** and **1**–**4** complexes in $CHCl_3$ at 25 °C.[a]

	Tetramethoxy-*p*-benzoquinone (**3**)	
	$\mathbf{1}_{\alpha\alpha\alpha\alpha}$	$\mathbf{1}_{\alpha\alpha\alpha\beta}$
K_a [M^{-1}]	$(9.4 \pm 0.1) \times 10^3$	$(3.5 \pm 0.1) \times 10^2$
ΔG° [kcal mol^{-1}]	-5.4 ± 0.1	-3.5 ± 0.1
ΔH° [kcal mol^{-1}]	-10.6 ± 0.3	-9.0 ± 0.3
$T\Delta S^\circ$ [kcal mol^{-1}]	-5.2 ± 0.3	-5.5 ± 0.3
	2,3-dimethoxy-*p*-benzoquinone (**4**)	
	$\mathbf{1}_{\alpha\alpha\alpha\alpha}$	$\mathbf{1}_{\alpha\alpha\alpha\beta}$
K_a [M^{-1}]	$(6.7 \pm 0.1) \times 10^3$	$(1.8 \pm 0.1) \times 10^2$
ΔG° [kcal mol^{-1}]	-3.9 ± 0.1	-3.1 ± 0.1
ΔH° [kcal mol^{-1}]	-9.1 ± 0.2	-8.0 ± 0.1
$T\Delta S^\circ$ [kcal mol^{-1}]	-5.2 ± 0.2	-4.9 ± 0.1

[a] Association constants were determined from UV/vis titrimetric measurements. Thermodynamic parameters were calculated from van't Hoff plots in the range 4–35 °C.

groups available for hydrogen bonding, respectively, and guests **3** and 2,3-dimethoxy-*p*-benzoquinone (**4**) can form at most four and three hydrogen bonds with host porphyrins, respectively, as shown in Scheme 4. Consequently, in the

0947-6539/98/0407-1268 $ 17.50+.50/0 *Chem. Eur. J.* **1998**, *4*, No. 7

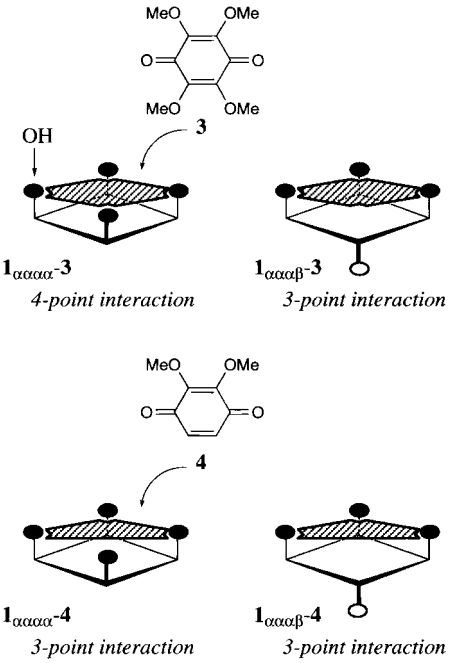

Scheme 4. Modes of interaction between porphyrin **1** and quinones **3** and **4**.

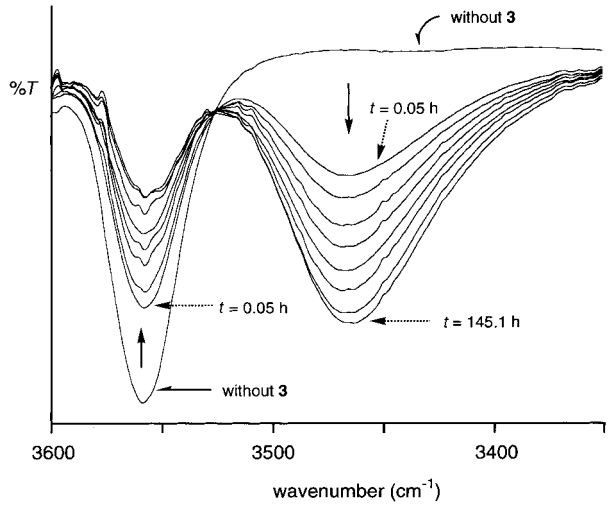

Figure 3. Time-dependent changes in the transmittance T in the IR spectrum of the OH bands of porphyrin **1** in the presence of quinone **3**. $t = 0.05$, 4.1, 9.1, 15.1, 21.3, 32.1, 84.3, 145.1 h after the addition of **3**. [**1**] = 1.0 mM, [**3**] = 3.2 mM in $CDCl_3$ at 298 K.

complexation of $\mathbf{1}_{\alpha\alpha\alpha\alpha}$ with **3**, large negative free energy and enthalpy changes were observed with a large association constant of $K_{a(\mathbf{1}_{\alpha\alpha\alpha\alpha}-\mathbf{3})} = (9.4 \pm 0.1) \times 10^3\ M^{-1}$ in $CHCl_3$ at 25 °C, indicating the formation of multiple hydrogen bonds.[14] In contrast, the binding affinities of $\mathbf{1}_{\alpha\alpha\alpha\alpha}-\mathbf{4}$, $\mathbf{1}_{\alpha\alpha\alpha\beta}-\mathbf{3}$ and $\mathbf{1}_{\alpha\alpha\alpha\beta}-\mathbf{4}$ are smaller than for the $\mathbf{1}_{\alpha\alpha\alpha\alpha}-\mathbf{3}$ complex, because the number of interaction sites is less. Therefore, the ratio of the two association constants $K_{a(\mathbf{1}_{\alpha\alpha\alpha\alpha}-\mathbf{3})}$ and $K_{a(\mathbf{1}_{\alpha\alpha\alpha\beta}-\mathbf{3})}$ is larger than that of $K_{a(\mathbf{1}_{\alpha\alpha\alpha\alpha}-\mathbf{4})}$ and $K_{a(\mathbf{1}_{\alpha\alpha\alpha\beta}-\mathbf{4})}$; $K_{a(\mathbf{1}_{\alpha\alpha\alpha\alpha}-\mathbf{3})}/K_{a(\mathbf{1}_{\alpha\alpha\alpha\beta}-\mathbf{3})} = 26.9$ and $K_{a(\mathbf{1}_{\alpha\alpha\alpha\alpha}-\mathbf{4})}/K_{a(\mathbf{1}_{\alpha\alpha\alpha\beta}-\mathbf{4})} = 3.7$. It is noteworthy that the binding behavior depends strictly on the number of hydrogen-bonded sites.[15]

Induced-fit molecular recognition between 1 and quinone: The atropisomeric interconversion initiated by addition of **3** to **1** was monitored by IR and ^1H NMR spectroscopy. In the presence of 3.2 equivalents of **3**, the IR spectrum of **1** showed OH bands at 3552 cm^{-1}, attributable to a free OH stretching vibration, and at 3464 cm^{-1}, assignable to a hydrogen-bonded OH vibration, as shown in Figure 3. After addition of **3**, the intensity of the latter band increased and that of the former decreased, suggesting that the hydrogen-bonded **1**–**3** complex gradually forms in the solution.

Figure 4 shows the ^1H NMR spectrum of **1** in $CDCl_3$ in the absence and presence of **3**. Signals from one of the phenyl protons (H_o) appeared at $\delta = 7.62 - 7.97$ and, in the absence of **3,** were not assignable to any atropisomer (Figure 4-Ia). Upon addition of a slight excess of **3** to a solution of **1**, six doublet signals assignable to the H_o protons appeared separately (Figure 4-Ib). One of these doublets gradually increased and other five decreased in intensity over a period of several days (Figure 4-Ic and d). At equilibrium, the strongest doublet peak remaining is identical to that obtained from a mixture of the isolated $\mathbf{1}_{\alpha\alpha\alpha\alpha}$ and **3** (Figure 4-Ie). In the region of the two *meta*-phenyl protons at $\delta = 7.06 - 7.23$ (H_m and $H_{m'}$), one doublet–doublet and one doublet signal were observed at equilibrium. These peaks are also assignable to $\mathbf{1}_{\alpha\alpha\alpha\alpha}$ protons upon complexation with **3**. OH signals from **1** are shown in Figure 4-II. Although OH protons gave one broad resonance peak, the addition of **3** resulted in peak splitting, attributable to each atropisomer (Figure 4-IIb).[16] Only one signal increased in intensity with time. The sharp signal observed at $\delta = 6.62$, is also assignable to OH protons from $\mathbf{1}_{\alpha\alpha\alpha\alpha}$. The spectra of the NH protons from the pyrrole residues in **1** also revealed the same behavior as described above (Figure 4-III). Furthermore, we confirmed that each proton signal assigned to $\mathbf{1}_{\alpha\alpha\alpha\beta}$ after addition of **3** is consistent with the spectrum obtained from a mixture of isolated $\mathbf{1}_{\alpha\alpha\alpha\beta}$ and **3.** Unlike the other three atropisomers, this complex exhibits three different sets of resonances for the *meso* aryl protons and OH protons, owing to the lower symmetry of $\mathbf{1}_{\alpha\alpha\alpha\beta}$.[17]

The changes in the relative amounts of each atropisomer in the presence of **3** are illustrated in Figure 5. Upon addition of **3** (3 equiv) to a solution of **1** in $CDCl_3$ at 25 °C, the proportion of $\mathbf{1}_{\alpha\alpha\alpha\alpha}$, which is a measure of the total amount of free and complexed host,[18] increased from 11% to 78%. In contrast, the proportion of $\mathbf{1}_{\alpha\alpha\alpha\beta}$ reached a peak of approximately 60% after 8 hours and then decreased to 17% thereafter. The proportions of the other two isomers, $\mathbf{1}_{\alpha\alpha\beta\beta}$ and $\mathbf{1}_{\alpha\beta\alpha\beta}$, gradually decreased with the increase of $\mathbf{1}_{\alpha\alpha\alpha\alpha}$. These results clearly demonstrate the dynamic process of induced-fit molecular recognition between the flexible host **1** and guest molecule **3**.

Figure 6a shows the temperature-dependent interconversion to $\mathbf{1}_{\alpha\alpha\alpha\alpha}$. At 43 °C, the addition of 1 equivalent of **3** to the porphyrin solution induced rapid atropisomerization to $\mathbf{1}_{\alpha\alpha\alpha\alpha}$; however, the proportion at equilibrium was only 39%. The total amount of $\mathbf{1}_{\alpha\alpha\alpha\alpha}$ at equilibrium increased with decreasing temperature. Furthermore, the interconversion of $\mathbf{1}_{\alpha\alpha\alpha\alpha}$ also depended on the concentration of quinone as shown in Figure 6b. The proportion of $\mathbf{1}_{\alpha\alpha\alpha\alpha}$ at equilibrium increased with increasing concentration of **3.** At 25 °C the addition of

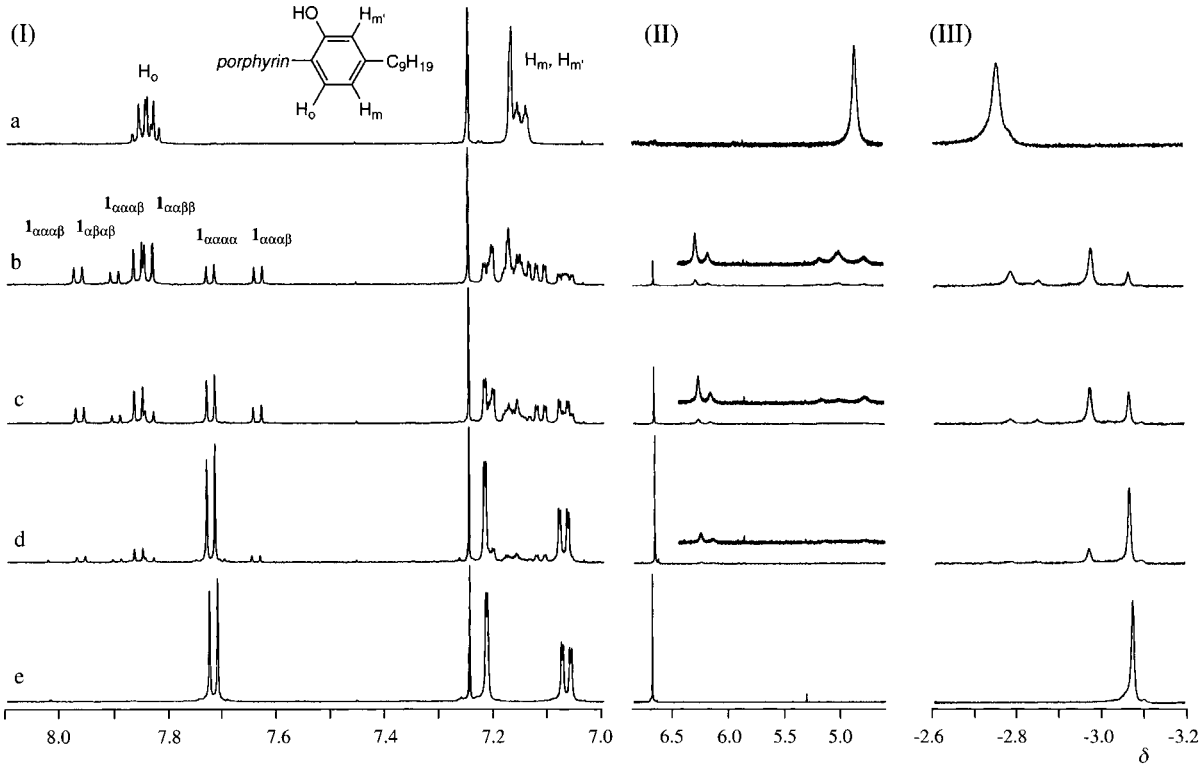

Figure 4. ^{1}H NMR spectra (500 MHz) of a mixture of **1** and **3** in $CDCl_3$ at 25 °C. (I) Protons attached to phenyl in **1**, (II) OH protons and (III) inner NH protons; a) before addition of **3**, b) 0.4 h, c) 23 h, and d) 479 h after addition of **3**; [**1**] = 2.4 mM, [**3**] = 7.2 mM; e) ^{1}H NMR spectrum of a mixture of isolated $\mathbf{1}_{aaaa}$ and **3**.

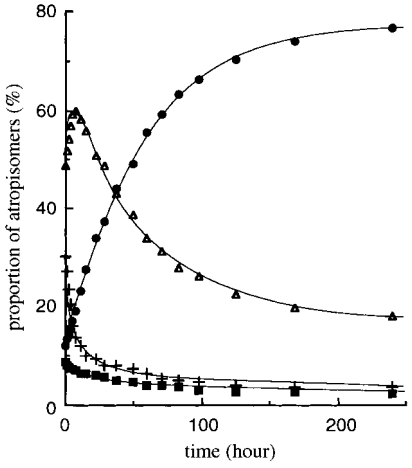

Figure 5. Kinetics of formation and decay of the four atropisomers of **1** upon addition of **3** in $CDCl_3$ at 25 °C; $\mathbf{1}_{aaaa}$ (●), $\mathbf{1}_{aaa\beta}$ △, $\mathbf{1}_{aa\beta\beta}$ (+), $\mathbf{1}_{a\beta a\beta}$ ■. [**1**] = 2.4 mM, [**3**] = 7.2 mM.

0.5, 1, and 5 equivalents of **3** yielded 36 %, 58 % and 80 % of $\mathbf{1}_{aaaa}$, respectively, at equilibrium in $CDCl_3$.

Comparisons of the relative amounts of the four atropisomers at equilibrium in the presence of **3** or **4** are shown in Figure 7. Addition of **4** to the porphyrin solution also changed the proportions of each isomer, but the drastic enhancement of the total amount of $\mathbf{1}_{aaaa}$ obtained with a mixture of **1** and **3** was not observed. These sharp differences are reflected in the binding affinities for the $\mathbf{1}_{aaaa}$–quinone and $\mathbf{1}_{aaa\beta}$–quinone complexes. Thus, the total amount of $\mathbf{1}_{aaaa}$ at equilibrium is clearly controlled by the thermodynamic stability of the **1**–quinone complex.

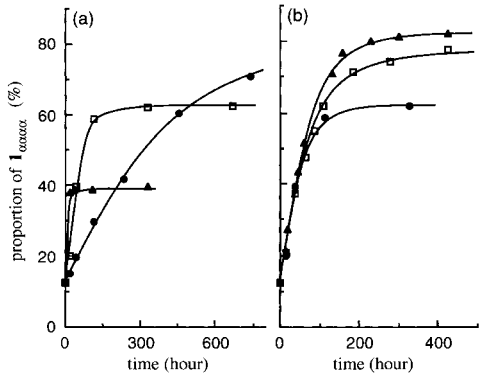

Figure 6. Comparison of the relative amounts of $\mathbf{1}_{aaaa}$ on addition of **3** in $CDCl_3$; a) at 43 °C (▲), at 23 °C (□) and at 9 °C (●), [**1**] = [**3**] = 2.4 mM; b) at 25 °C and [**1**] = 2.4 mM, [**3**] = 24 mM (▲), [**3**] = 7.2 mM (□) and [**3**] = 2.4 mM (●).

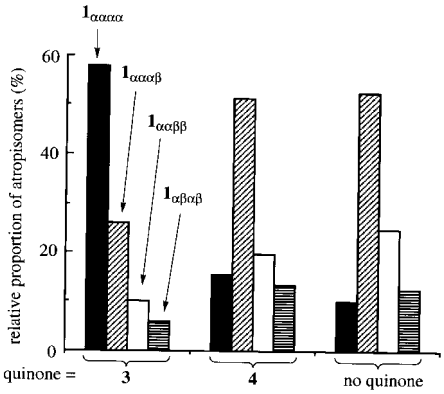

Figure 7. Comparison of the relative amounts of atropisomers $\mathbf{1}_{aaaa}$, $\mathbf{1}_{aaa\beta}$, $\mathbf{1}_{aa\beta\beta}$, and $\mathbf{1}_{a\beta a\beta}$ on addition of **3** or **4** after reaching equilibrium at 25 °C in $CDCl_3$. [**1**] = [**3**] = [**4**] = 2.4 mM.

0947-6539/98/0407-1270 $ 17.50+.50/0 *Chem. Eur. J.* **1998**, *4*, No. 7

Mechanism of induced-fit molecular recognition: A plausible mechanism for the guest-induced structural changes in the host **1** is shown in Scheme 5. Since the relative amounts of the four atropisomers of **1** in the absence of quinone are close to the statistical ratio ($\mathbf{1}_{\alpha\alpha\alpha\alpha}$:$\mathbf{1}_{\alpha\alpha\alpha\beta}$:$\mathbf{1}_{\alpha\alpha\beta\beta}$:$\mathbf{1}_{\alpha\beta\alpha\beta}$ = 1:4:2:1), each kinetic process for atropisomeric interconversion is defined by k, $2k$, or $4k$ (Scheme 5), where k represents the rate

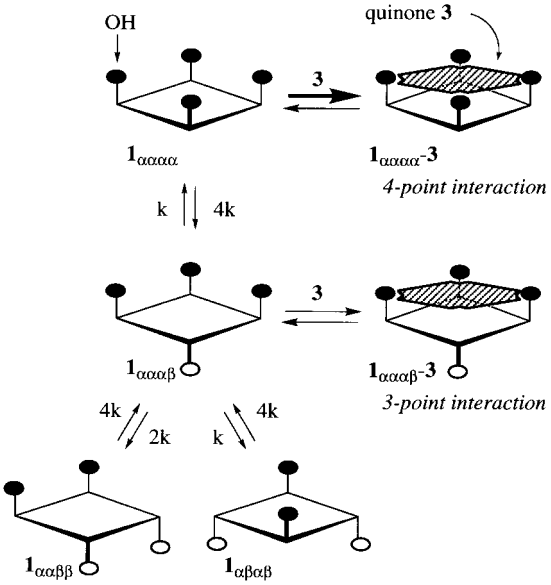

Scheme 5. Proposed mechanism of induced-fit molecular recognition between porphyrin **1** and tetramethoxy-*p*-benzoquinone **3**.

constant for internal rotation about one C(aryl)–C(porphyrin) bond. Assuming that the affinities of $\mathbf{1}_{\alpha\alpha\beta\beta}$–quinone and $\mathbf{1}_{\alpha\beta\alpha\beta}$–quinone pairs are negligibly small, the kinetic and equilibrium equations which represent the induced-fitting process are defined in Equations (1)–(6), where Q is quinone,

$$d([\mathbf{1}_{\alpha\alpha\alpha\alpha}] + [\mathbf{1}_{\alpha\alpha\alpha\alpha}\text{–Q}])/dt = -4k[\mathbf{1}_{\alpha\alpha\alpha\alpha}] + k[\mathbf{1}_{\alpha\alpha\alpha\beta}] \quad (1)$$

$$d([\mathbf{1}_{\alpha\alpha\alpha\beta}] + [\mathbf{1}_{\alpha\alpha\alpha\beta}\text{–Q}])/dt = 4k([\mathbf{1}_{\alpha\alpha\alpha\alpha}] - [\mathbf{1}_{\alpha\alpha\alpha\beta}] + [\mathbf{1}_{\alpha\alpha\beta\beta}] + [\mathbf{1}_{\alpha\beta\alpha\beta}]) \quad (2)$$

$$d([\mathbf{1}_{\alpha\alpha\beta\beta}])/dt = -4k[\mathbf{1}_{\alpha\alpha\beta\beta}] + 2k[\mathbf{1}_{\alpha\alpha\alpha\beta}] \quad (3)$$

$$d([\mathbf{1}_{\alpha\beta\alpha\beta}])/dt = -4k[\mathbf{1}_{\alpha\beta\alpha\beta}] + k[\mathbf{1}_{\alpha\alpha\alpha\beta}] \quad (4)$$

$$K_{a(\mathbf{1}_{\alpha\alpha\alpha\alpha}\text{–Q})} = [\mathbf{1}_{\alpha\alpha\alpha\alpha}\text{–Q}]/([\mathbf{1}_{\alpha\alpha\alpha\alpha}][Q]) \quad (5)$$

$$K_{a(\mathbf{1}_{\alpha\alpha\alpha\beta}\text{–Q})} = [\mathbf{1}_{\alpha\alpha\alpha\beta}\text{–Q}]/([\mathbf{1}_{\alpha\alpha\alpha\beta}][Q]) \quad (6)$$

and $[\mathbf{1}_{\alpha\alpha\alpha\alpha}\text{–Q}]$ and $[\mathbf{1}_{\alpha\alpha\alpha\beta}\text{–Q}]$ represent the concentration of $\mathbf{1}_{\alpha\alpha\alpha\alpha}$–Q and $\mathbf{1}_{\alpha\alpha\alpha\beta}$–Q complexes, respectively. The dynamic process derived from the computer-generated curves based on Equations (1)–(6) with several parameters, k, K_a, and initial proportions of each isomer, is consistent with the observed data, as shown in Figures 8 and 9.[19] Thus, these results demonstrate that induced-fit molecular recognition occurs through the combination of multiple equilibria associated with host–guest complexation and internal rotation.

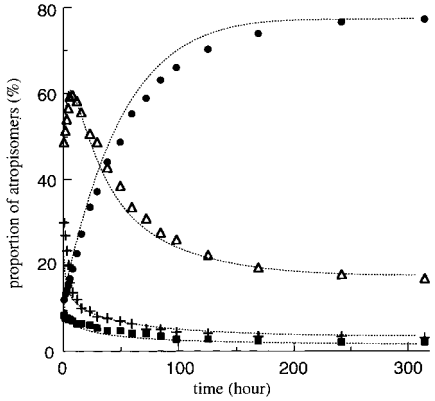

Figure 8. Experimental and simulated results for the atropisomerization of **1** upon addition of **3**. The lines represent the simulation curves calculated from Equations (1)–(6). [**1**] = 2.4 mM, [**3**] = 7.2 mM in $CDCl_3$ at 25 °C. $\mathbf{1}_{\alpha\alpha\alpha\alpha}$ (●), $\mathbf{1}_{\alpha\alpha\alpha\beta}$ (△), $\mathbf{1}_{\alpha\alpha\beta\beta}$ (+), $\mathbf{1}_{\alpha\beta\alpha\beta}$ (■).

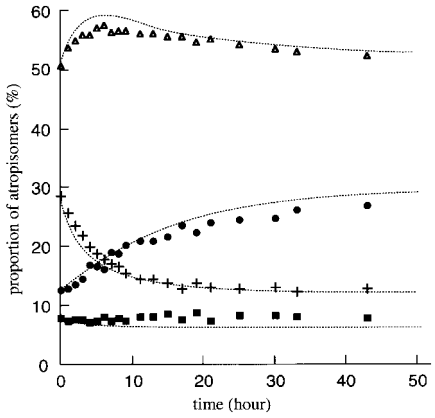

Figure 9. Experimental and simulated results for the atropisomerization of **1** upon addition of **4**. The lines represent the simulation curves calculated from Equations (1)–(6). [**1**] = 2.4 mM, [**4**] = 7.2 mM in $CDCl_3$ at 25 °C. $\mathbf{1}_{\alpha\alpha\alpha\alpha}$ (●), $\mathbf{1}_{\alpha\alpha\alpha\beta}$ (△), $\mathbf{1}_{\alpha\alpha\beta\beta}$ (+), $\mathbf{1}_{\alpha\beta\alpha\beta}$ (■).

Interaction between metalloporphyrin and quinone: To investigate the effect of internal rotation on the induced fitting, molecular recognition behavior, we selected two metalloporphyrin derivatives of **1**. The rate constants of internal rotation about one C(aryl)–C(porphyrin) bond for the nickel and zinc complexes **1**·**Ni** and **1**·**Zn** were determined by NMR spectroscopy and HPLC analysis, respectively. Atropisomerization of **1**·**Zn** is slower than that of free base **1**. Decay of $\mathbf{1}_{\alpha\alpha\alpha\alpha}$·**Zn** was monitored by analytical HPLC and took place with a rate constant of $(6.9 \pm 0.4) \times 10^{-7}\ s^{-1}$ at 25 °C. In contrast, the internal rotation about the C(aryl)–C(porphyrin) bond in **1**·**Ni** was too fast for analysis of the rate of atropisomerization by the same method, so the rate constant for **1**·**Ni** was estimated to be $> 1 \times 10^{-3}\ s^{-1}$ by variable-temperature NMR spectroscopy. These results indicate that the atropisomerization of **1**·**Ni** occurs more rapidly than that of free base **1** and the slowest rate is found for **1**·**Zn**; thus the internal rotation depends on the metal substituent in the center of the porphyrin core. According to X-ray crystallographic analysis for several metalloporphyrins, the porphyrin core, which contains four pyrrole nitrogen atoms, is planar for the zinc complex, whereas nickel porphyrin adopts a puckered conformation.[20, 21] If the atropisomerization due

to internal rotation about porphyrin–aryl bonds proceeds through the nonplanar, puckered conformation as a reaction intermediate, the rotational energy barrier for **1·Ni** should be smaller than that for **1·Zn**. The dependence of the internal rotation on the metal observed here is consistent with previous work reported by Whitten and Freitag.[22]

The affinities of **1·Zn** and **1·Ni** for **3** are shown in Table 2. Association constants of $\mathbf{1}_{\alpha\alpha\alpha\alpha}\cdot\mathbf{Zn}$ and $\mathbf{1}_{\alpha\alpha\alpha\beta}\cdot\mathbf{Zn}$ complexes with **3** were determined by UV/visible titrimetric analysis of the isolated atropisomers. In the case of **1·Ni**, we estimated the association constants from the peak areas for each atropisomer and quinone in the ^{1}H NMR spectrum. The association constants of $\mathbf{1}_{\alpha\alpha\alpha\alpha}\cdot\mathbf{Zn}$ and $\mathbf{1}_{\alpha\alpha\alpha\alpha}\cdot\mathbf{Ni}$ complexes with **3** are larger than those for $\mathbf{1}_{\alpha\alpha\alpha\beta}\cdot\mathbf{Zn}$ and $\mathbf{1}_{\alpha\alpha\alpha\beta}\cdot\mathbf{Ni}$ respectively, but are slightly smaller than that for free base $\mathbf{1}_{\alpha\alpha\alpha\alpha}$ with **3**.

Table 2. Association constants K_a of porphyrins for quinone **3** at 25 °C in $CHCl_3$.

	K_a [M^{-1}]	
	$\alpha\alpha\alpha\alpha$-isomer	$\alpha\alpha\alpha\beta$-isomer
free base **1**[a]	$(9.4\pm0.1)\times10^3$	$(3.5\pm0.1)\times10^2$
zinc complex **1**·Zn[a]	$(3.2\pm0.1)\times10^3$	$(1.6\pm0.1)\times10^2$
nickel complex **1**·Ni[b]	$(2.7\pm0.6)\times10^3$	$(1.6\pm0.4)\times10^2$

[a] Determined by UV/vis titration. [b] Determined by ^{1}H NMR analysis; assuming that the complex formations of $\mathbf{1}_{\alpha\alpha\beta\beta}$–**3** and $\mathbf{1}_{\alpha\beta\alpha\beta}$–**3** are negligible, the concentrations of **1** and **1**–**3** are estimated from comparison of each isomer's peak area in OH protons.

The changes in the relative amounts of each atropisomer of **1·Ni** and **1·Zn** in the presence of **3** were also monitored by ^{1}H NMR spectroscopy and the results are plotted in Figure 10.

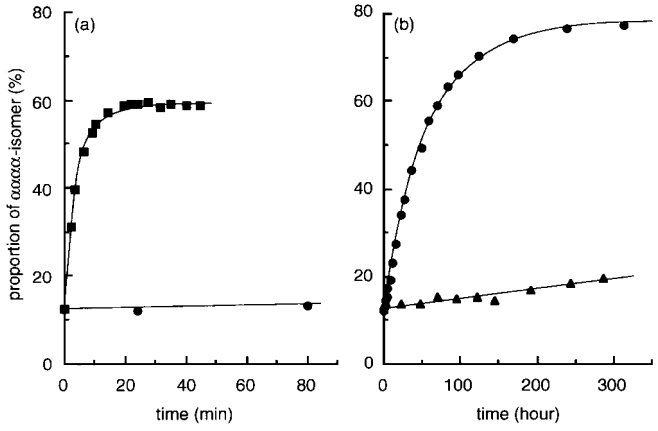

Figure 10. Changes in the relative amounts of atropisomers $\mathbf{1}_{\alpha\alpha\alpha\alpha}\cdot\mathbf{Ni}$ (■), $\mathbf{1}_{\alpha\alpha\alpha\alpha}$ (●), and $\mathbf{1}_{\alpha\alpha\alpha\alpha}\cdot\mathbf{Zn}$ (▲) with time, upon addition of **3** in $CDCl_3$ at 25 °C. [**1·Ni**] = [**1**] = [**1·Zn**] = 2.4 mM, [**3**] = 7.2 mM.

Surprisingly, the increase of $\mathbf{1}_{\alpha\alpha\alpha\alpha}\cdot\mathbf{Ni}$ was extremely rapid and the proportion of the $\alpha\alpha\alpha\alpha$-atropisomer reached 60% within 10 min after the addition of **3** to a solution of **1·Ni** in $CDCl_3$. In contrast, the atropisomerization of **1·Zn** was quite slow compared with that of free base **1** or **1·Ni**. These sharp differences demonstrate that the atropisomerization induced by quinone is governed by the rate of rotation about the C(aryl)–C(porphyrin) bonds.

Although the rate constant for internal rotation and the two association constants, $K_{a(\mathbf{1}_{\alpha\alpha\alpha\alpha}\cdot\mathbf{Ni}-\mathbf{3})}$ and $K_{a(\mathbf{1}_{\alpha\alpha\alpha\beta}\cdot\mathbf{Ni}-\mathbf{3})}$, cannot be completely determined for **1·Ni** complexes by the direct methods employed for free base **1** because of difficulties inherent in isolating each atropisomer, least-squares optimization of the experimental data with the damped Gauss-Newton algorithm leads to these parameters. The four curves calculated from Equations (1)–(4) (Figure 11) fit the data

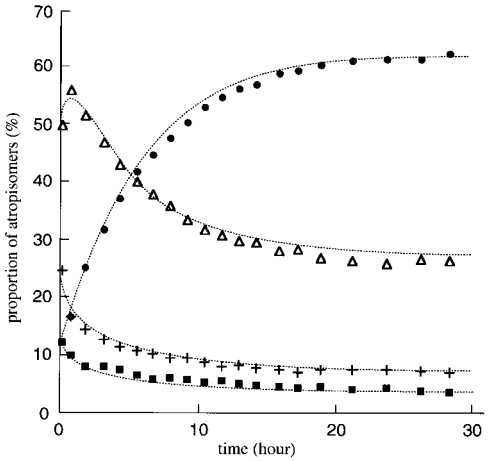

Figure 11. Comparisons of best fits to Equations (1)–(4) with experimental data for the atropisomerization of **1·Ni** upon addition of **3**. [**1·Ni**] = 2.4 mM, [**3**] = 7.2 mM in $CDCl_3$ at 25 °C. $\mathbf{1}_{\alpha\alpha\alpha\alpha}\cdot\mathbf{Ni}$ (●), $\mathbf{1}_{\alpha\alpha\alpha\beta}\cdot\mathbf{Ni}$ (△), $\mathbf{1}_{\alpha\alpha\beta\beta}\cdot\mathbf{Ni}$ (+), $\mathbf{1}_{\alpha\beta\alpha\beta}\cdot\mathbf{Ni}$ (■). Initial isomer contents are 12.5, 50.0, 25.0, and 12.5%, respectively.

well and give the following kinetic and thermodynamic parameters: $k=(4.9\pm0.2)\times10^{-3}$ s^{-1}, $K_{a(\mathbf{1}_{\alpha\alpha\alpha\alpha}\cdot\mathbf{Ni}-\mathbf{3})}=(2.3\pm0.1)\times10^3$ M^{-1} and $K_{a(\mathbf{1}_{\alpha\alpha\alpha\beta}\cdot\mathbf{Ni}-\mathbf{3})}=(1.2\pm0.1)\times10^2$ M^{-1}. The association constants obtained from the fitting are consistent with those estimated from ^{1}H NMR spectroscopy (Table 2). The agreement between the observed data and the curve fitting indicates that the atropisomerization of **1·Ni** in the presence of **3** follows the route described in Scheme 5, and the rapid isomerization to $\mathbf{1}_{\alpha\alpha\alpha\alpha}\cdot\mathbf{Ni}$ derives from the large rate constant for internal rotation in nickel porphyrin. However, the proportion of $\mathbf{1}_{\alpha\alpha\alpha\alpha}\cdot\mathbf{Ni}$ at equilibrium is only 60%, suggesting that the ratio of association constants $K_{(\mathbf{1}_{\alpha\alpha\alpha\alpha}\cdot\mathbf{Ni}-\mathbf{3})}$ and $K_{(\mathbf{1}_{\alpha\alpha\alpha\beta}\cdot\mathbf{Ni}-\mathbf{3})}$ is relatively small compared with that in free base **1**; $K_{a(\mathbf{1}_{\alpha\alpha\alpha\alpha}\cdot\mathbf{Ni}-\mathbf{3})}/K_{a(\mathbf{1}_{\alpha\alpha\alpha\beta}\cdot\mathbf{Ni}-\mathbf{3})}=19.2$, whereas $K_{a(\mathbf{1}_{\alpha\alpha\alpha\alpha}-\mathbf{3})}$ and $K_{a(\mathbf{1}_{\alpha\alpha\alpha\beta}-\mathbf{3})}=26.9$.

Conclusions

These results indicate that the atropisomerization of porphyrin to the $\alpha\alpha\alpha\alpha$-form is induced by binding of the guest molecule to the host porphyrin through hydrogen bonds. Simulation of the dynamic process based on the multiple equilibrium system in Scheme 5 with the kinetic and thermodynamic parameters k and K_a is consistent with the observed data. It supports the view that: a) the driving force for induced-fitting behavior is the difference between $K_{a(\mathbf{1}_{\alpha\alpha\alpha\alpha}-Q)}$ and $K_{a(\mathbf{1}_{\alpha\alpha\alpha\beta}-Q)}$ and b) the rate of conversion to the $\alpha\alpha\alpha\alpha$-form

0947-6539/98/0407-1272 $ 17.50+.50/0 *Chem. Eur. J.* **1998**, *4*, No. 7

is dominated by the inherent rate of internal rotation about C(aryl)–C(porphyrin) bonds.

It is known that the ligand-induced internal rotation about a chemical bond in an enzyme framework is quite an important factor in the rearrangement of interaction sites upon ligand binding, as shown in Scheme 1b. This may be the initiation step in enzymatic reactions and/or signal transformation. In the present study, we have demonstrated the existence of a dynamic molecular recognition process upon binding between host and guest molecules, with internal rotation about a C–C bond. In this system, induced-fit molecular recognition can be quantitatively analyzed using kinetic and thermodynamic parameters. This analysis helps our understanding of the rearrangement of functional groups resulting from binding between an enzyme and ligand.

Experimental Section

Instrumentation: ^{1}H and ^{13}C NMR spectra were obtained by means of JEOL A-500, GX-400 or FX-90Q spectrometers and chemical shifts were reported relative to residual $CHCl_3$ at $\delta = 7.24$. Mass spectra were measured in FAB mode with a JEOL JMS-SX102A spectrometer. UV/visible spectra were recorded on a Hitachi U-3410 spectrophotometer or a Hewlett–Packard 8452A diode array spectrophotometer with a cell compartment kept at constant temperature. IR spectra were measured with a Perkin–Elmer 2000 FT-IR spectrometer.

Materials: Analytical TLC was performed on precoated silica gel Merck $60F_{254}$. [D]Chloroform was purchased from Aldrich and used without further purification. The chloroform used for recording the UV/visible spectra was Aldrich ACS HPLC grade and contained 2-methyl-2-butene as a stabilizer.[14] Quinones **3** and **4** were prepared as described previously.[23, 24]

3-Nonylanisole (**5**): A solution of *n*-nonylmagnesium bromide (ca. 0.09 mol) in Et_2O (100 mL) was added dropwise to a solution of 3-bromoanisole (10 mL, 0.079 mol) and 1,3-bis(diphenylphosphino)propane nickel(II) chloride (214 mg, 0.395 mmol) in anhydrous Et_2O (20 mL) under N_2 at 0 °C. The reaction mixture was refluxed for 6 h and stirred at room temperature for 12 h. After the reaction had been quenched with 1N HCl (480 mL) at 0 °C, the organic layer was separated and the aqueous layer was extracted with Et_2O. The combined organic layer was washed sequentially with H_2O, saturated $NaHCO_3$(aq) solution, and H_2O. The solution was then dried over anhydrous $MgSO_4$. After removal of the solvent, the yellow residue was purified by distillation under reduced pressure (0.15 mm Hg, 107–115 °C) to afford 15.9 g (67.7 mmol, 86%) of **5**. ^{1}H NMR (90 MHz, $CDCl_3$): $\delta = 0.90$ (t, $J = 6$ Hz, 3H), 1.0–2.8 (m, 14H), 2.63 (t, $J = 7$ Hz), 3.80 (s, 3H), 6.6–7.3 (m, 4H).

2-Methoxy-4-nonylbenzaldehyde (**6**): A solution of dichloromethyl methyl ether (5.0 mL, 55 mmol) in anhydrous CH_2Cl_2 (150 mL) was added dropwise over 6 h to a solution of **5** (4.64 g, 19.8 mmol) and $TiCl_4$ (8.7 mL, 79 mmol) in anhydrous CH_2Cl_2 at −78 °C. After reaching room temperature, the reaction mixture was poured into ice-cold water and the organic layer was separated. The aqueous layer was extracted with CH_2Cl_2, and the combined organic layer was washed with H_2O, saturated $NaHCO_3$(aq) solution, and saturated NaCl(aq) solution. The product was dried over anhydrous $MgSO_4$, filtered, and concentrated under reduced pressure. The remaining yellow liquid was purified by column chromatography on silica gel (hexane:benzene = 2:1) to afford 2.06 g (7.85 mmol, 40%) of **6**. ^{1}H NMR (90 MHz, $CDCl_3$): $\delta = 0.90$ (t, $J = 6$ Hz, 3H), 1.3–1.7 (m, 14H), 2.67 (t, $J = 7$ Hz), 3.93 (s, 3H), 6.86 (d, $J = 7$ Hz, 1H), 6.89 (s, 1H), 7.73 (d, $J = 7$ Hz, 1H), 10.40 (s, 1H).

***meso*-Tetrakis(2-methoxy-4-nonylphenyl)porphyrin** (**7**): Pyrrole (530 μL, 0.77 mmol), boron trifluoride diethyl etherate (310 μL, 2.5 mmol), and anhydrous ethanol (5.8 μL) were added successively to a solution of **6** (2.02 g, 0.77 mmol) in anhydrous toluene (770 mL) at room temperature. After the reaction mixture had been stirred at room temperature for 2.5 h, 2,3-dichloro-5,6-dicyano-1,4-benzoquinone (1.73 g, 7.63 mmol) was added and the mixture was stirred at room temperature for 2 h. The solution was then neutralized by addition of triethylamine (360 μL, 2.6 mmol). After removal of the solvent under reduced pressure, the crude product was purified by column chromatography on basic alumina (toluene) to afford 751 mg (0.606 mmol, 32%) of an atropisomeric mixture of **7**. TLC: R_f (hexane:ethyl acetate = 5:1) = 0.21, 0.42, 0.56 and 0.64. ^{1}H NMR spectroscopy of a mixture of the four atropisomers (400 MHz, $CDCl_3$): $\delta = -2.63$ (br s, 2H), 0.92 (t, $J = 7.0$ Hz, 12H), 1.26–1.58 (m, 48H), 1.90 (quintet, $J = 7.6$ Hz, 8H), 2.92 (t, $J = 7.8$ Hz, 8H), 3.52, 3.55 and 3.58 (s, total 12H), 7.1–7.2 (m, 8H), 7.81, 7.82, 7.86 and 7.91 (d, $J = 7.2$, 7.3, 7.3 and 7.5 Hz, respectively, total 4H), 8.72 (m, 8H).

***meso*-Tetrakis(2-hydroxy-4-nonylphenyl)porphyrin** (**1**): The atropisomeric mixture of **7** (0.78 g, 0.63 mmol) was dissolved in anhydrous CH_2Cl_2 (40 mL) and the solution was cooled to 0 °C under N_2. A solution of BBr_3 (0.1M, 6.3 mL) in CH_2Cl_2 was added dropwise, and the reaction mixture was stirred at 0 °C for 3 h and then at room temperature for 16 h. The reaction was quenched by addition of ice-cold water at 0 °C and the organic layer was separated. The aqueous layer was extracted with CH_2Cl_2 and the combined organic layer was washed with H_2O, saturated $NaHCO_3$(aq) and saturated NaCl(aq) solutions. After drying over anhydrous Na_2SO_4, the solution was filtered, and concentrated under reduced pressure to give a crude, purple product. The residue was purified by column chromatography on silica gel (hexane:ethyl acetate = 4:1) to afford 700 mg (0.587 mmol, 94%) of an atropisomeric mixture of **8**. TLC: R_f(hexane-ethyl acetate = 4:1) = 0.11 for $\mathbf{1}_{\alpha\alpha\alpha\alpha}$, 0.52 for $\mathbf{1}_{\alpha\alpha\alpha\beta}$ and 0.73 for $\mathbf{1}_{\alpha\alpha\beta\beta}$ and $\mathbf{1}_{\alpha\beta\alpha\beta}$. ^{1}H NMR spectroscopy of a mixture of the four atropisomers (400 MHz, $CDCl_3$): $\delta = -2.75$ (s, 2H), 0.92 (t, $J = 6.9$ Hz, 12H), 1.25-1.58 (m, 48H), 1.90 (m, 8H), 2.90 (t, $J = 7.7$ Hz, 8H), 4.84 (br s, 4H), 7.14–7.17 (m, 8H), 7.81–7.85 (m, 4H), 8.91 (s, 8H); ^{13}C NMR spectroscopy of a mixture of the four atropisomers (125 MHz, $CDCl_3$):[25, 26] $\delta = 14.16$, 22.76, 29.44, 29.55, 29.67, 29.68, 30.09, 31.34, 31.98, 36.08, 113.56–113.69, 115.22–115.34, 119.89–119.96, 124.64–124.57, 134.75–134.91, 146.00–146.06, 155.14–155.22; MS-FAB$^+$: $m/z = 1183$ [M^++1]; HRMS-FAB$^+$: calcd for $C_{80}H_{102}N_4O_4$ [M^+] 1182.7901, found 1182.7930.

Isolation of $\mathbf{1}_{\alpha\alpha\alpha\alpha}$ and $\mathbf{1}_{\alpha\alpha\alpha\beta}$: The atropisomeric mixture of **1** (ca. 5 mg) was dissolved in $CHCl_3$, placed on a TLC plate and developed with hexane/ethyl acetate (3:1) as the eluent at 4 °C over 20 min. The $\alpha\alpha\alpha\alpha$-atropisomer, $\mathbf{1}_{\alpha\alpha\alpha\alpha}$, which was the most polar isomer, was easily separated from the other three atropisomers. The fractions corresponding to $\mathbf{1}_{\alpha\alpha\alpha\alpha}$ were combined and eluted with ethyl acetate. The eluent was evaporated immediately over an ice-bath under reduced pressure. The isomer $\mathbf{1}_{\alpha\alpha\alpha\beta}$ was obtained using the same procedure. The purities of the isolated isomers were determined by reversed-phase HPLC to be 95% and 90%, respectively. ^{1}H NMR spectroscopy of $\mathbf{1}_{\alpha\alpha\alpha\alpha}$ in the presence of **3** (500 MHz, $CDCl_3$): $\delta = -3.075$ (s, 2H), 0.918 (t, $J = 7.1$ Hz, 12H), 1.216–1.583 (m, 8H), 1.879–1.940 (m, 8H), 2.903 (t, $J = 7.7$ Hz, 8H), 6.644 (s, 4H), 7.072 (dd, $J = 1.7$ Hz, 7.4 Hz, 4H), 7.219 (d, $J = 1.7$ Hz, 4H), 7.720 (d, $J = 7.4$ Hz, 4H), 8.904 (s, 8H); ^{1}H NMR spectroscopy of $\mathbf{1}_{\alpha\alpha\alpha\beta}$ in the presence of **3** (500 MHz, $CDCl_3$): $\delta = -3.02$ (s, 2H), 0.92 (t, $J = 7.2$ Hz, 12H), 1.2–1.6 (m, 8H), 1.83–1.97 (m, 8H), 2.91 (t, $J = 7.5$ Hz, 8H), 4.78 (s, 1H), 6.35 (s, 1H), 6.48 (s, 2H), 7.05 (dd, $J = 1.7$ Hz, 7.6 Hz, 1H), 7.11 (dd, $J = 1.7$ Hz, 7.7 Hz, 2H), 7.16 (m, 1H), 7.18 (dd, $J = 1.7$ Hz, 7.6 Hz, 1H), 7.20–7.22 (m, 3H), 7.61 (d, $J = 7.6$ Hz, 1H), 7.86 (d, $J = 7.6$ Hz, 2H), 7.98 (d, $J = 7.6$ Hz, 1H), 8.88-8.94 (m, 8H).

***meso*-Tetrakis(2-hydroxy-4-nonylphenyl)porphyrin zinc(II) complex** (**1·Zn**): A solution of $Zn(OAc)_2 \cdot 2H_2O$ (28 mg, 0.13 mmol) in MeOH (3 mL) was added to a solution of **1** (91 mg, 0.077 mmol) in $CHCl_3$ (14 mL). The mixture was refluxed for 20 min, cooled to room temperature, and poured into H_2O. The organic layer was separated and the aqueous layer was extracted with Et_2O. The combined organic layer was washed with H_2O and dried over anhydrous Na_2SO_4. The solution was filtered and concentrated under reduced pressure to give 95.5 mg (quant) of **1·Zn**. ^{1}H NMR spectroscopy of a mixture of the four atropisomers (500 MHz, $CDCl_3$): $\delta = 0.923$ (t, $J = 6.7$ Hz, 12H), 1.27–1.59 (m, 48H), 1.83–1.95 (m, 8H), 2.80–2.94 (m, 8H), 4.36, 4.62, 4.67, 4.76, 4.81 and 4.85 (br s, total 4H), 6.65–7.16 (m, 8H), 7.72-7.86 (a mixture of doublets, 4H), 8.76–8.97 (a mixture of ABq and singlet, 8H); ^{13}C NMR spectroscopy of a mixture of the four atropisomers (125 MHz, $CDCl_3$):[26] $\delta = 14.176$, 22.776, 29.47, 29.63, 29.70, 29.72, 31.35, 32.01, 32.01, 113.68–114.41, 114.76–114.98, 119.74–119.80, 124.97–125.31, 132.14–132.42, 134.64–134.88, 145.42–145.65,

150.39 – 150.88, 154.39 – 154.80; MS-FAB$^+$: 1245 [M^+]; HRMS-FAB$^+$: calcd for $C_{80}H_{100}N_4O_4{}^{64}Zn$ [M^+] 1244.7036, found 1244.6968.

***meso*-Tetrakis(2-hydroxy-4-nonylphenyl)porphyrin nickel(II) complex (1·Ni)**: A solution of $Ni(OAc)_2 \cdot 4H_2O$ (48 mg, 0.19 mmol) in MeOH (4 mL) was added to a solution of **1** (90 mg, 0.076 mmol) in $CHCl_3$ (20 mL). The mixture was refluxed for 45 min, cooled to room temperature, and poured into H_2O. The organic layer was separated and the aqueous layer was extracted with Et_2O. The combined organic layer was washed with H_2O and dried over anhydrous Na_2SO_4. The solution was filtered and concentrated under reduced pressure to give 90 mg (0.073 mmol, 92 %) of **1·Ni**. ^{1}H NMR spectroscopy of a mixture of the four atropisomers (500 MHz, $CDCl_3$): $\delta = 0.906$ (t, $J = 7.0$ Hz, 12H), 1.26 – 1.64 (m, 48H), 1.81 – 1.89 (m, 8H), 2.83 – 2.86 (m, 8H), 4.72, 4.73, 4.74, 4.75, 4.77, 4.77 (s, total 4H), 7.07 – 7.13 (m, 8H), 7.64 – 7.68 (a mixture of doublets, total 4H), 8.81 (s, 8H); ^{13}C NMR spectroscopy of a mixture of the four atropisomers (125 MHz, $CDCl_3$):[26] $\delta = 14.18$, 22.78, 29.47, 29.64, 29.70, 29.72, 31.35, 32.01, 36.08, 113.56 – 113.98, 114.07 – 114.95, 119.71 – 119.82, 124.91 – 125.36, 132.06 – 132.46, 134.51 – 134.87, 145.19 – 145.62, 150.24 – 150.85, 153.38 – 154.75; MS-FAB$^+$: 1239 [M^+]; HRMS-FAB$^+$: calcd for $C_{80}H_{100}N_4O_4{}^{58}Ni$ [M^+] 1238.7098, found 1238.7114.

Binding studies: All UV/visible binding studies were carried out on a Hewlett – Packard 8452A diode array spectrophotometer with $CHCl_3$ containing 2-methyl-2-butene as a stabilizer. Initially, a porphyrin solution (2.0 mL, [porphyrin] = $10^{-5} - 10^{-4}$ M) was poured into a 1 cm quartz cell. The UV/visible spectrum of the pure host solution was recorded, and some of the stock quinone solution (e.g. 10 μL) was transferred into the cell with a syringe. The spectrum was recorded and the process was repeated until the desired guest-to-host ratio was obtained. The parameters from the changes in monitored absorbance were calculated using a nonlinear curve-fitting procedure based on the damped Gauss – Newton method.

Determination of the relative amounts of each atropisomer: All NMR spectroscopy studies were carried out on a JEOL A-500 NMR spectrometer using $CDCl_3$ without further purification. A solution of porphyrin and quinone was placed in a 5 mm NMR spectroscopy tube under Ar and sealed. The tube was maintained in a bath held at constant temperature ($\pm$ 1 °C) and measurements were taken at regular time intervals.

Acknowledgements: This work was supported by a Grant-in-Aid of Specially Promoted Research (No. 04101003) from the Ministry of Education, Science, and Culture (Japan). F.M.B. (Johannes Gutenberg University, Mainz) gratefully acknowledges financial support from the Deutscher Akademischer Austauschdienst (DAAD) under the program for Integrated Studies Abroad, during his stay at Kyoto University in 1993 – 1994. T.H. thanks Prof. Y. Hisaeda from Kyushu University for his warm encouragement during the preparation of this article.

Received: January 7, 1998 [F953]

[1] D. J. Cram, *Angew. Chem.* **1988**, *100*, 1041; *Angew. Chem. Int. Ed. Engl.* **1988**, *27*, 1009.

[2] a) D. E. Koshland, Jr., *Proc. Natl. Acad. Sci. USA* **1958**, *44*, 98; b) D. E. Koshland, Jr., *Angew. Chem.* **1994**, *106*, 2468; *Angew. Chem. Int. Ed. Engl.* **1994**, *33*, 2375.

[3] a) T. A. Steitz, M. L. Ludwig, F. A. Quiocho, W. N. Lipscomb, *J. Biol. Chem.* **1967**, *242*, 4662; b) W. S. Bennett, R. Huber, *Crit. Rev. Biochem.* **1984**, *15*, 291; c) M. Gerstein, A. M. Lesk, C. Chothia, *Biochemistry* **1994**, *33*, 6739.

[4] a) C.-W. Chen, H. W. Whitlock, Jr., *J. Am. Chem. Soc.* **1978**, *100*, 4921; b) J. Rebek, Jr., B. Askew, M. Killoran, D. Nemeth, F.-T. Lin, *J. Am. Chem. Soc.* **1987**, *109*, 2426; c) J. C. Adrian, C. S. Wilcox, *J. Am. Chem. Soc.* **1989**, *111*, 8055; d) G. M. Sanders, M. van Dijk, B. M. Machiels, A. van Veldhuizen, *J. Org. Chem.* **1991**, *56*, 1301; e) C. Vicent, S. C. Hirst, F. Garcia-Tellado, A. D. Hamilton, *J. Am. Chem. Soc.* **1991**, *113*, 5466; f) R. P. Sijbesma, R. J. M. Nolte, *J. Am. Chem. Soc.* **1991**, *113*, 6695; g) J. C. Adrian, Jr., C. S. Wilcox, *J. Am. Chem. Soc.* **1992**, *114*, 1398; h) R. Güther, M. Nieger, F. Vögtle, *Angew. Chem.* **1993**, *105*, 647; *Angew. Chem. Int. Ed. Engl.* **1993**, *32*, 601; i) M. M. Conn, G. Deslongchamps, J. de Mendoza, J. Rebek, Jr., *J. Am. Chem. Soc.* **1993**, *115*, 3548; j) M. Fujita, F. Ibukuro, H. Hagihara, K. Ogura, *Nature* **1994**, *367*, 720; k) D. V. Stynes, *Inorg. Chem.* **1994**, *33*, 5022; l) F. Würthner, J. Rebek, Jr., *Angew. Chem.* **1995**, *107*, 503; *Angew. Chem. Int. Ed. Engl.* **1995**, *34*, 446; m) M. Fujita, S. Nagao, K. Ogura, *J. Am. Chem. Soc.* **1995**, *117*, 1649; n) H. L. Anderson, S. Anderson, J. K. M. Sanders, *J. Chem. Soc. Perkin Trans. 1* **1995**, 2231; o) R. M. Grotzfeld, N. Branda, J. Rebek, Jr., *Science* **1996**, *271*, 487; p) I. Vernik, D. V. Stynes, *Inorg. Chem.* **1996**, *35*, 6210; q) A. V. Eliseev, M. I. Nelen, *J. Am. Chem. Soc.* **1997**, *119*, 1147; r) M. A. Houghton, A. Bilyk, M. M. Harding, P. Turner, T. W. Hambley, *J. Chem. Soc. Dalton Trans.* **1997**, 2725.

[5] Recently, we have reported that *meso*-tetrakis(2-hydroxynaphthyl)-porphyrin (**2**) is a suitable ubiquinone receptor. The atropisomerization of **2** was not detected even in boiling toluene. T. Hayashi, T. Miyahara, N. Koide, Y. Kato, H. Masuda, H. Ogoshi, *J. Am. Chem. Soc.* **1997**, *119*, 7281.

[6] T. Hayashi, T. Asai, H. Hokazono, H. Ogoshi, *J. Am. Chem. Soc.* **1993**, *115*, 12210.

[7] L. K. Gottwald, E. F. Ullman, *Tetrahedron Lett.* **1969**, 3071.

[8] C. M. Elliott, *Anal. Chem.* **1980**, *52*, 666.

[9] J. Lindsey, *J. Org. Chem.* **1980**, *45*, 5215.

[10] Several groups have described a thermal shift in the equilibrium of atropisomers at high temperatures. See for example: a) N. Nishino, K. Kobata, H. Mihara, T. Fujimoto, *Chem. Lett.* **1992**, 1991; b) E. Rose, M. Quelquejeu, C. Pochet, N. Julien, A. Kossanyi, L. J. Hamon. *Org. Chem.* **1993**, *58*, 5030; c) J. Setsune, M. Hashimoto, *J. Chem. Soc. Chem. Commun.* **1994**, 657; d) E. Rose, A. Cardon-Pilotaz, M. Quelquejeu, N. Bernard, A. Kossanyi, B. Desmazières, *J. Org. Chem.* **1995**, *60*, 3919.

[11] Y. Kuroda, A. Kawashima, Y. Hayashi, H. Ogoshi, *J. Am. Chem. Soc.* **1997**, *119*, 4929.

[12] M. Kumada, K. Tamao, K. Sumitani, *Org. Synth.* **1978**, *58*, 127.

[13] The rate constant for internal rotation about the C(aryl) – C(porphyrin) bond in Ullman's porphyrin, *meso*-tetrakis(2-hydroxyphenyl)porphyrin, is $1.5 \pm 0.5 \times 10^{-5}$ s^{-1} in methanol at 23 °C.[7]

[14] In the previous paper, association constants were determined in chloroform containing trace amounts of ethanol as a stabilizer.[6] However, ethanol can act as a competitive inhibitor in the formation of hydrogen-bonded complexes. In this paper, we used chloroform containing 2-methyl-2-butene as a stabilizer to obtain the thermodynamic parameters.

[15] T. Hayashi, T. Miyahara, Y. Aoyama, M. Kobayashi, H. Ogoshi, *Pure Appl. Chem.* **1994**, *66*, 797.

[16] The downfield shift of the OH protons shown in Figure 4-IIb depends on the degree of hydrogen bonding of the OH groups.

[17] M. J. Crossley, L. D. Field, A. J. Forster, M. M. Harding, S. Sternhell, *J. Am. Chem. Soc.* **1987**, *109*, 341.

[18] In the NMR spectroscopy study, the peak area of proton resonance corresponding with the host porphyrin is a measure of the total concentration of ($[\mathbf{1}_{\alpha\alpha\alpha\alpha}] + [\mathbf{1}_{\alpha\alpha\alpha\alpha} - Q]$) and ($[\mathbf{1}_{\alpha\alpha\alpha\beta}] + [\mathbf{1}_{\alpha\alpha\alpha\beta} - Q]$), respectively, since the exchange process between the free and complexed host molecule is fast on the NMR time scale.

[19] If direct atropisomeric equilibrium between $\mathbf{1}_{\alpha\alpha\alpha\alpha} - Q$ and $\mathbf{1}_{\alpha\alpha\alpha\beta} - Q$ without intermediate dissociation to porphyrin and quinone is assumed in this system, the simulated curves for the relative amounts of each atropisomer cannot be reconciled with the kinetic data shown in Figure 8 and 11.

[20] J. L. Hoard, in *Porphyrins and Metalloporphyrins*, (Ed.: K. M. Smith), Elsevier, Amsterdam, **1975**, p. 317.

[21] R. G. Alden, B. A. Crawford, R. Doolen, M. R. Ondrias, J. A. Shelnutt, *J. Am. Chem. Soc.* **1989**, *111*, 2070.

[22] R. A. Freitag, D. G. Whitten, *J. Phys. Chem.* **1983**, *87*, 3918.

[23] H. Orita, M. Shimizu, T. Hayakawa, K. Takehira, *Bull. Chem. Soc. Jpn.* **1989**, *62*, 1652.

[24] M. H. Akhtar, A. Begleiter, D. Johnson, W. Lown, L. McLaughlin, S.-K. Sim, *Can. J. Chem.* **1975**, *53*, 2891.

[25] C_α carbons of the four pyrrole rings were not detected, owing to the broadening derived from N – H tautomerism.

[26] Several singlet peaks appear at the same position for each phenyl and pyrrole carbon, owing to the presence of a mixture of four atropisomers.